Deep tissue flowmetry based on diffuse speckle contrast analysis

Renzhe Bi, Jing Dong, and Kijoon Lee*

School of Chemical and Biomedical Engineering, Nanyang Technological University, Singapore 637457
**Corresponding author: KJLee@ntu.edu.sg*

Received September 28, 2012; revised January 9, 2013; accepted March 18, 2013;
posted March 25, 2013 (Doc. ID 177034); published April 24, 2013

Diffuse correlation spectroscopy (DCS) is an emerging modality for noninvasive deep tissue blood flow monitoring that is becoming increasingly popular; it conducts an autocorrelation analysis of fast fluctuating photon count signals from a single speckle. In this Letter, we show that the same level of deep tissue flow information can be obtained from a much simpler analysis on the spatial distribution of the speckles that is obtained by a CCD camera, which we named diffuse speckle contrast analysis (DSCA). Both the flow phantom experiment and *in vivo* cuff occlusion data are presented. DSCA can be considered a new optical modality that combines DCS and laser speckle contrast imaging (LSCI), which exploits simple instrumentation and analysis and yet is sensitive to deep tissue flow.

OCIS codes: (030.6140) Speckle; (170.6480) Spectroscopy, speckle; (290.1990) Diffusion.
http://dx.doi.org/10.1364/OL.38.001401

Diffuse correlation spectroscopy (DCS) is a noninvasive technique to obtain the relative blood flow (rBF) in deep tissue; it has already been widely adopted in clinical studies in muscle and brain [1,2]. Taking advantage of low power near-infrared (NIR) laser and the flexible geometry of the source and detector, DCS is particularly suitable for *in vivo* bedside monitoring study on human subjects, including infants.

In typical DCS systems, rBF is extracted from temporal autocorrelation function of the fluctuating transmission signal, which is normally obtained by a hardware correlator [3] or a counter board together with an FFT-based software correlator [4]. Both methods need a very sensitive detector, such as a photon-counting avalanche photodiode and photomultiplier tube, and multiple detectors are needed for concurrent multichannel operation. Thus a typical DCS setup is relatively expensive, especially for multiple-channel detectors, which is necessary to achieve depth-selective flow measurement.

To provide an alternative approach for rBF measurement in deep tissue, we propose a diffuse speckle contrast analysis (DSCA) method, which estimates the flow value based on the analysis of the speckle pattern in spatial domain. In this system, we use the same light source as a typical DCS system, which is a long-coherence-length NIR laser coupled to a multimode fiber. But a high-sensitivity CCD camera is used instead of the photon-counting detector. The CCD takes an image of a small area on the surface of the subject, to acquire the diffuse laser speckle pattern, from which we can obtain the rBF of certain depth.

In the traditional DCS system, the electric field autocorrelation function $G_1(\vec{r},\tau)$ is used to characterize temporal fluctuations, which satisfies the correlation diffusion equation [5]

$$\left(-\frac{1}{3\mu_s'}\nabla^2+\mu_a+\frac{1}{3}\alpha\mu_s'k_0^2\langle\Delta r^2(\tau)\rangle\right)G_1(\vec{r},\tau)=S(\vec{r}), \quad (1)$$

where k_0 is the wavenumber of the light in medium, α is the fraction of moving scatterers out of total scatterers, $\langle r^2(\tau)\rangle$ represents the mean square displacement of the moving scatterers after a delay time τ. In practice, the intensity autocorrelation function $G_2(\vec{r},\tau)$ is measured from experiment instead of $G_1(\vec{r},\tau)$. The Siegert relation, $g_2(\tau)=1+\beta|g_1(\tau)|^2$, relates the two autocorrelation functions, where $g_1(\tau)$ and $g_2(\tau)$ are normalized versions of electric field and intensity autocorrelation function, respectively, and β is a constant related to the ratio between the detector size and the speckle size. In short, the blood flow index is derived from temporal autocorrelation from one single speckle in DCS.

Meanwhile, flow-induced speckle fluctuations will also result in the reduction of laser speckle contrast in space for a given exposure time. The speckle contrast is defined as the ratio of the standard deviation to the mean intensity across many detectors or pixels, $K_s=\sigma_s/\langle I\rangle$, where the subscript s refers to the spatial, as opposed to temporal, variations [6,7]. In laser speckle contrast imaging (LSCI), the relationship between K_s and $g_1(\tau)$ is well studied, as shown in the equation below for normalized intensity variance V in terms of the exposure time T [8,9].

$$V(T)=[K_s(T)]^2=\frac{2}{T}\int_0^T(1-\tau/T)[g_1(\tau)]^2\mathrm{d}\tau. \quad (2)$$

In LSCI a wide field illumination is used rather than point illumination, and $g_1(\tau)$ is commonly assumed as a simple exponential form. Thus, normal LSCI is suitable for flow imaging of a superficial layer inside a relatively transparent medium. Note that Eq. (2) holds in general cases where $g_1(\tau)$ might deviate from simple exponential decay, although it has been most useful in single scattering situation so far.

Both DCS and LSCI technologies have been around for decades, and were combined for dynamical properties measurement recently [10]; however, to the authors' knowledge, there has been little study to apply laser speckle contrast analysis (LASCA) in deep tissue flow measurement. In this Letter, we will show that with point NIR laser source illumination, LASCA can also be used to study the change of flow dynamics inside a deep layer of highly scattering medium. This can also be regarded as an alternative approach of conventional DCS.

Comparison between the proposed DSCA setup and traditional DCS setup is made in Fig. 1. DSCA shares the same light source as the DCS system, which is fiber-coupled point illumination of long coherence length laser. However, in contrast to the traditional DCS, which uses single-mode fiber as a detector, DSCA uses a lens-coupled CCD chip to take images of the speckle pattern on the surface of the sample. The banana-shaped sensitivity volume for a source–detector pair is shown in Fig. 1 (shaded region). Although the sensitivity volume in Fig. 1(b) spreads more near the detector, we can divide the CCD image into small segments and treat each segment as a separate detector, which has a sensitivity volume similar to the one shown in Fig. 1(a). Since the CCD image covers a relatively large area, we can acquire multichannel detection from a single exposure by this segmentation.

According to Eq. (2), K_s of the speckle pattern on the sample's surface is determined by $g_1(\tau)$ of the same position, which can be derived from Eq. (1) in semi-infinite geometry under Brownian motion assumption. If we define the sample surface as $z = 0$, Green's function solution of the correlation diffuse equation is given by [11]

$$G_1(r,\tau) = \frac{3\mu_s'}{4\pi}\left[\frac{\exp(-k_D(\tau)r_1)}{r_1} - \frac{\exp(-k_D(\tau)r_2)}{r_2}\right], \quad (3)$$

where $k_D(\tau) = \sqrt{3\mu_s'\mu_a + 6\mu_s'^2 k_0^2 \alpha D_B \tau}$, $r_1 = \sqrt{r^2 + z_0^2}$, $r_2 = \sqrt{r^2 + (z_0 + 2z_b)^2}$ and r is source–detector separation, $z_0 = 1/\mu_s'$, $z_b = 2(1 - R_{\text{eff}})/3\mu_s'(1 + R_{\text{eff}})$, where R_{eff} represents effective reflection coefficient.

The normalized $G_1(r,\tau)$, which is given by

$$g_1(r,\tau) = G_1(r,\tau)/G_1(r,0), \quad (4)$$

will be used in Eq. (2). Therefore, within the same medium, K_s is determined by flow rate, source–detector separation, and exposure time.

To validate the DSCA method, we designed a flow-phantom experiment. Details about the in-house phantom building were described in our previous work [4]. The optical properties of the solid body were $\mu_s' = 8\ \text{cm}^{-1}$ and $\mu_a = 0.03\ \text{cm}^{-1}$. The hollow tube was filled up with small beads to randomize the flow direction.

The experimental setup is shown in Fig. 2. The light source was a continuous wave laser with a long coherence length (>10 m) operating at 785 nm (DL785-100-S, ~100 mW, CrystaLaser, Reno, Nevada, USA). An EMCCD (Cascade 512F, Photometrics) was used as detector. A $f = 35$ mm biconvex lens was used as an imaging lens, with a magnification of 1, and a lens tube (not shown in figure) was used along the light path between the sample and CCD to prevent exposure to stray lights. The EMCCD chip size, which was the same as the imaging area, was about 8 mm × 8 mm, where the individual pixel size was 16 μm × 16 μm. The imaging region covered a source–detector separation range from 1.6 to 2.4 cm, within which the sensitivity volume of larger separation overlapped more with the flow region in phantom (see Fig. 2). For the control experiment the other surface of the phantom was used, where the minimum distance from the surface to the flow cylinder is 3 cm, with the same source–detector geometry.

During the experiment, Lipofundin N 20% (B. Braun Melsungen AG, Germany) with a concentration of 0.6% was pumped through the cylindrical tube at different rates, ranging from 0 to 0.10 ml/s in steps of 0.02 ml/s. The light source and detector were placed on the upper surface of the phantom, and 10 images were taken for every single flow rate (exposure time, 0.1 ms). For comparison, the same protocol was applied on the lower side instead of the upper side of the phantom, so that sensitivity volume does not overlap with the actual flow. We kept all the conditions the same as the actual flow experiment, including the flow rate, in order to examine the effect of sensitivity volume only.

For better illustration of the data acquisition and processing in DSCA system, Fig. 2 also shows the raw speckle image from the imaging area and the processed K_s distribution. The raw speckle images are normalized by the smooth intensity background, which is averaged over 100 speckle images. K_s is calculated from every segment of 100(vertical) × 50(horizontal) pixels, and the processed speckle contrast distribution is shown at the top right part in Fig. 2. Thus, we have 10 different source–detector separations from each row.

Our main results are summarized in Fig. 3. According to the numerical simulation of Eq. (2), over a large range, $1/K_s^2$ tends to be linear as the blood flow index ($= \alpha D_b$ in Brownian motion model) as shown in Fig. 3(a). Figure 3(b) shows experimental $1/K_s^2$ values as a function of flow rate for two different situations. When the flow region is within the sensitivity volume, $1/K_s^2$ increases as flow rate increases (blue line). On the other hand, with the same source–detector separation, when the flow depth is out of the sensitivity volume, $1/K_s^2$ is not affected by the flow rate (black line). Thus, we

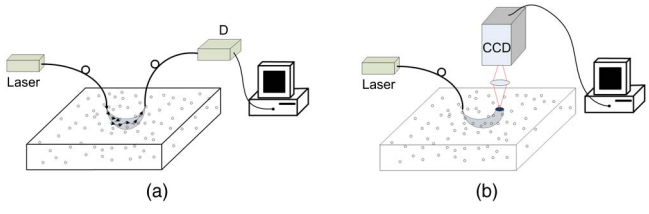

Fig. 1. (a) Schematic of a traditional DCS setup, where D is a photon counting detector and a hardware correlator. (b) Schematic of DSCA setup, where the CCD camera takes images of the speckle pattern on the sample surface. The shaded region in the sample represents the sensitivity volume of the source–detector pair.

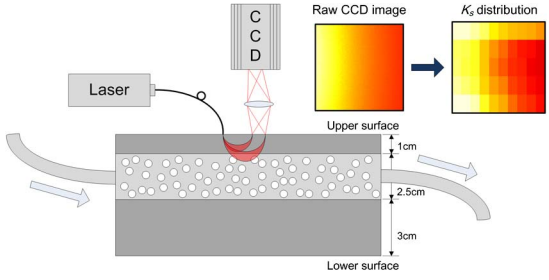

Fig. 2. Schematic of the flow-controlled phantom experiment. Speckle images, before and after the processing, are shown in pseudocolor. See text for details.

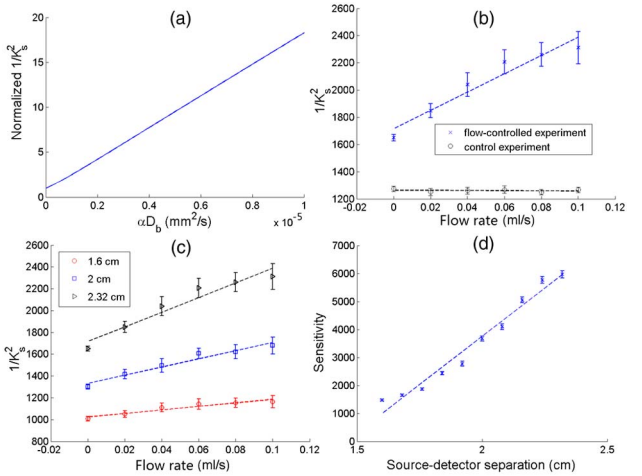

Fig. 3. Summary of simulated and experimental data. (a) Numerical simulation of $1/K_s^2$ as a function of αD_b, with exposure time T of 0.1 ms. (b) $1/K_s^2$ plotted against flow rate, for comparison between the flow depth inside and outside the sensitivity volume, at the same source–detector separation of 2.32 cm. (c) $1/K_s^2$ as a function of the flow rate for 3 source–detector separations. The slope can be regarded as the sensitivity to the flow rate. (d) Flow sensitivities measured at 10 different source–detector separations.

can confirm the DSCA system is only sensitive to the flow within the sensitivity volume. To quantify the flow sensitivity, we plot in Fig. 3(c) the dependence of $1/K_s^2$ on the flow rate for different source–detector separations, where the slope can be regarded as the sensitivity to the flow rate. It nicely shows that $1/K_s^2$ behaves linearly over a broad range of the imaging area, and the sensitivity increases as source–detector separation increases. The flow sensitivities calculated from all 10 available source–detector separations in a single CCD image are plotted in Fig. 3(d), where it is clearly shown that the larger overlap with the flow region results in higher sensitivity to the flow. This demonstrates that multidepth measurements can be conveniently achieved by single exposure in the DSCA system, which may enable a depth-specific measurement of deep tissue blood flow.

To validate the biomedical application of DSCA system, we also performed *in vivo* experiments on a human arm together with a normal time-domain DCS system [4] simultaneously, sharing the same light source and source–detector separation of 1.8 cm. The imaging rate of our DSCA system could reach up to 30 Hz, while the update rate of the DCS system was 1 Hz. Moving windows average was applied with a window size of 4. Our protocol included three periods: baseline, cuff occlusion with pressure of 200 mmHg, and release.

$1/K_s^2$, which is used as the indicator for blood flow dynamics in DSCA system, is obtained from an area of 50 × 50 pixels. Good correlation between the rBF measured by the normal DCS system and the DSCA system is demonstrated in Fig. 4. We note that the DSCA result may seem to have poorer SNR than the DCS result, but the fluctuations in the DSCA result have periodicity with ~0.1 Hz frequency, which corresponds to the normal low-frequency oscillation (LFO) in blood flow regulation. LFO cannot be detected by DCS due to its much lower time resolution.

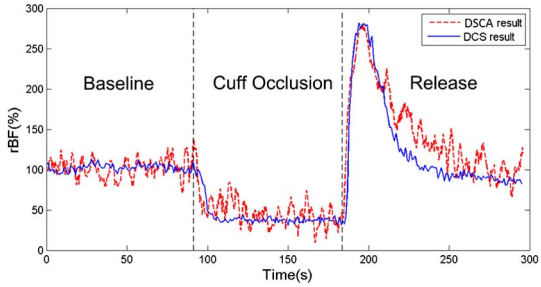

Fig. 4. Simultaneous measurement of rBF by DCS and DSCA systems during arm cuff occlusion protocol.

Similar to LSCI, exposure time plays an important role in the DSCA system. From reported *in vivo* DCS results on human limbs, $g_1(\tau)$ is most sensitive to rBF in $\tau = 0.02 \sim 1$ ms range [4,11]. We chose 0.1 ms as the exposure time in the DSCA experiments, considering the balance between SNR and speckle contrast. Compared with LSCI, a relatively bigger averaging pixel number is necessary to guarantee the accuracy of K_s, possibly compromising the imaging resolution. If needed, higher imaging magnification can be used to overcome the resolution issue, although it will shorten the span of source–detector separation.

In conclusion, by combining with diffuse correlation theory, we applied LASCA in rBF measurement inside deep tissue for the first time. Compared to the DCS system, our DSCA system has significantly reduced the cost, increased the sampling rate, and simplified the analysis. We validated its performance using a flow phantom and human arm cuff occlusion protocol. The inherent multichannel measurement capability may find applications in real-time depth-sensitive flow measurement.

This work was supported by the Singapore Ministry of Education under the Academic Research Fund Tier 1 grant RG37/07.

References

1. E. M. Buckley, N. M. Cook, T. Durduran, M. N. Kim, C. Zhou, R. Choe, G. Q. Yu, S. Shultz, C. M. Sehgal, D. J. Licht, P. H. Arger, M. E. Putt, H. Hurt, and A. G. Yodh, Opt. Express **17**, 12571 (2009).
2. G. Q. Yu, T. Durduran, G. Lech, C. Zhou, B. Chance, E. R. Mohler, and A. G. Yodh, J. Biomed. Opt. **10**, 024027 (2005).
3. Y. Shang, Y. Q. Zhao, R. Cheng, L. X. Dong, D. Irwin, and G. Q. Yu, Opt. Lett. **34**, 3556 (2009).
4. J. Dong, R. Bi, J. H. Ho, P. S. P. Thong, K.-C. Soo, and K. Lee, J. Biomed. Opt. **17**, 097004 (2012).
5. D. A. Boas and A. G. Yodh, J. Opt. Soc. Am. A **14**, 192 (1997).
6. J. D. Briers and S. Webster, J. Biomed. Opt. **1**, 174 (1996).
7. A. F. Fercher and J. D. Briers, Opt. Commun. **37**, 326 (1981).
8. R. Bandyopadhyay, A. S. Gittings, S. S. Suh, P. K. Dixon, and D. J. Durian, Rev. Sci. Instrum. **76**, 093110 (2005).
9. D. A. Boas and A. K. Dunn, J. Biomed. Opt. **15**, 011109 (2010).
10. T. B. Rice, S. D. Konecky, A. Mazhar, D. J. Cuccia, A. J. Durkin, B. Choi, and B. J. Tromberg, J. Opt. Soc. Am. A **28**, 2108 (2011).
11. T. Durduran, R. Choe, W. B. Baker, and A. G. Yodh, Rep. Prog. Phys. **73**, 076701 (2010).